

Phenomenological description of the parton-parton interaction in high-transverse-momentum collisions*

Ephraim Fischbach and George W. Look

Department of Physics, Purdue University, West Lafayette, Indiana 47907

(Received 26 July 1976)

A phenomenological quark-quark scattering model is presented which reproduces the inclusive high-transverse-momentum data from CERN ISR and Fermilab for the processes $pp \rightarrow cX$ and $pn \rightarrow cX$, where $c = \pi^\pm, \pi^0, K^\pm, p, \bar{p}$. This model is obtained by multiplying the usual parton-parton scattering amplitude by the factor $(1 - \hat{t}/B)^{-2}$ where $-\hat{t}$ is the square of the gluon 4-momentum and $B = 18 \text{ GeV}^2$. The single parameter B describes both the x_1 dependence at constant s and the s (or p_\perp) dependence at constant x_1 for all c at all energies. An additional normalization constant is needed for each particle to fix the overall scale of the total cross section.

I. INTRODUCTION

Recently, the suggestion has been made¹⁻⁵ that the suppression of the strong-interaction cross sections, for processes in which particles with large transverse momenta are produced, might make it possible to detect weak-interaction effects in very-high-energy hadron-hadron collisions. This possibility would be realized if the weak cross section for a given process decreased less rapidly with increasing transverse momentum p_\perp than did the corresponding strong cross section. Under these circumstances the weak contribution becomes enhanced relative to the strong contribution, and this enhancement is reflected in a parameter such as \mathcal{O} , the longitudinal polarization of an outgoing proton, which increases with increasing p_\perp . Since \mathcal{O} is a measure of parity nonconservation, and hence of the weak contribution to the process in question, $\mathcal{O}(p_\perp)$ may be used to probe the weak hadron-hadron interaction at very high energies.

If we focus our attention on strangeness-conserving processes such as $pp \rightarrow pX$ (where X is a nonstrange hadronic state), then the weak and strong amplitudes add *coherently* and hence \mathcal{O} should be of order $(\sigma_w/\sigma_s)^{1/2}$, where σ_w and σ_s are the weak and strong cross sections, respectively. We emphasize that even in the parton model, where the observed cross section results from an *incoherent* sum of the contributions from individual parton-parton scattering processes, the contribution from any *single* parton-parton scattering is obtained by adding *coherently* the appropriate weak and strong amplitudes. It follows that the parton model for the weak and strong processes should be formulated in a similar way so as to reflect the coherence of the two processes at the level of the parton-parton interaction. This coherence, coupled with the previously discussed enhancement of the weak amplitude at large p_\perp , ac-

counts for the relatively large predicted values for \mathcal{O} , $|\mathcal{O}| \approx 10^{-3} - 10^{-4}$, that were found in Refs. 1-3. Given a knowledge of the weak and strong parton-parton scattering amplitudes, \mathcal{O} can be evaluated in a straightforward manner:

$$\mathcal{O} = \frac{E d\sigma^+ / d^3p - E d\sigma^- / d^3p}{E d\sigma^+ / d^3p + E d\sigma^- / d^3p}. \quad (1.1)$$

In Eq. (1.1) $E d\sigma^\pm / d^3p$ is the invariant differential cross section for producing a proton with energy $E \cong |\vec{p}|$ in a state of \pm helicity in the process $pp \rightarrow pX$. For inclusive production of pions (or any other particle) parity nonconservation is manifested through the asymmetry parameter \mathcal{Q} defined by

$$\mathcal{Q} = \frac{E d\sigma_+ / d^3p - E d\sigma_- / d^3p}{E d\sigma_+ / d^3p + E d\sigma_- / d^3p}. \quad (1.2)$$

In Eq. (1.2) $E d\sigma_\pm / d^3p$ is the invariant differential cross section for producing a pion from a proton with initial \pm helicity.

The difficulty in applying Eqs. (1.1) and (1.2) is that for the inclusive processes of interest, namely $pp \rightarrow pX$ and $pp \rightarrow \pi X$, no analytic expression for the strong parton-parton interaction currently exists which is valid over the whole range of kinematic variables for which experimental data are available. In the absence of such an expression approximate formulas for \mathcal{O} and \mathcal{Q} were derived,¹ assuming maximal constructive interference of the weak and strong amplitudes, which express these parameters in terms of the experimentally observed (strong) cross section σ_s :

$$\mathcal{O} \cong -\sqrt{2} \frac{(E d\sigma_w / d^3p)^{1/2}}{(E d\sigma_s / d^3p)^{1/2}}, \quad (1.3a)$$

$$\mathcal{Q} \cong \frac{(E d\sigma_{w^+} / d^3p)^{1/2} - (E d\sigma_{w^-} / d^3p)^{1/2}}{(E d\sigma_s / d^3p)^{1/2}}. \quad (1.3b)$$

In Eqs. (1.3) σ_w is the total cross section that would result from an unpolarized proton beam if only weak interactions were present, while σ_{w^\pm}

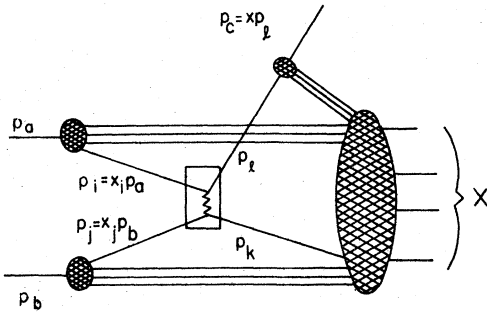


FIG. 1. Parton-model diagram for the strong process $p(p_a) + p(p_b) \rightarrow c(p_c) + X$. The boxed portion represents the strong parton-parton scattering process.

and σ_w are the corresponding cross sections if the initial proton beam is polarized with helicity ± 1 .

It would, of course, be preferable to calculate \mathcal{O} or \mathcal{Q} directly using the appropriate analytic expressions for the weak and strong parton-parton amplitudes τ_w and τ_s . The purpose of this paper is to present a simple phenomenological expression for τ_s which accurately describes the available strong-interaction data for the inclusive processes $pp \rightarrow pX, \pi X, KX$. Since the phase of τ_s is irrelevant in computing the invariant differential cross sections, we will take τ_s to be real and defer to a later paper a discussion of the relative phase of τ_s and τ_w . The starting point for our treatment of τ_s is the quark-quark scattering model of Berman, Bjorken, and Kogut⁶ (BBK), and in particular a simple modification of the single-vector-gluon exchange model discussed extensively by Ellis and Klinger.⁷ The quark-quark scattering mechanism is also the basis of the model of τ_w used in Ref. 1. In this model, shown in Fig. 1, the partons i and j interact via the exchange of a single (massless) vector gluon. Not surprisingly, this simple model does not adequately describe the data, especially the rapid decrease of the cross section with increasing p_{\perp} . We will show, however, that if the parton-parton amplitude is multiplied by a phenomenological function of the parton-parton momentum transfer \hat{t} given by

$$F^2(\hat{t}) = (1 - \hat{t}/B)^{-2}, \quad (1.4)$$

$$B = 18 \text{ GeV}^2$$

then the resulting theoretical expression describes the available data surprisingly well. This suggests that we calculate \mathcal{O} and \mathcal{Q} directly from Eqs. (1.1) and (1.2) by combining this expression for τ_s with the previously discussed model of τ_w .¹

Although the phenomenological expression for τ_s does indeed describe the data, it does not, of

course, represent a fundamental theory of high-energy inclusive scattering. If we imagine that the function $F^2(\hat{t})$ represents the effects of more complicated processes, such as multigluon exchanges, then a theory of inclusive scattering based on the quark-quark scattering mechanism can perhaps be constructed. Alternatively, we may try to interpret the expression in Eq. (1.4) as a quark form factor such as has been proposed by Chanowitz and Drell⁸ to account for the observed scaling violations in deep-inelastic ep scattering. For present purposes we will set such considerations aside and restrict our attention to phenomenological considerations.

In what follows we will focus exclusively on the effective-gluon (EG) model discussed above. There are, however, other models which have been considered, and we refer the reader to a summary of these given in Ref. 9. Among the most popular is the constituent-interchange model⁹ (CIM) which has enjoyed a measure of success in explaining the observed p_{\perp} dependence of inclusive cross sections. This is achieved in part by allowing different subprocesses to contribute to the production of mesons and baryons, and to the production of the same observed particles in different kinematic regions. Since the CIM and BBK mechanisms are qualitatively different, the CIM cannot be combined coherently with the weak model of Ref. 1, and so the CIM is not useful for our purposes. In addition, the simplicity of a single universal production mechanism is so appealing, especially from a computational point of view, that elaboration of the EG model is strongly suggested for its own sake.

In Sec. II the EG model is described in detail, and in Sec. III it is compared to experiment. It will be shown that this model accounts for the dependence of the inclusive cross sections on $x_{\perp} = 2p_{\perp}/\sqrt{s}$ (where \sqrt{s} = c.m. energy) as seen both at the CERN ISR for pp scattering¹⁰⁻¹³ and at Fermilab for p -nucleus scattering.¹⁴ The fits are only moderately sensitive to the value of the mass parameter B given in Eq. (1.4) with a range $B = (16-24) \text{ GeV}^2$ giving the best fits to the results of different experiments. The s dependence of the cross sections, or equivalently the p_{\perp} dependence at constant x_{\perp} , is also correctly represented with the exception of the p and \bar{p} s dependence extracted from p -nucleus scattering at Fermilab.¹⁴

After this work was completed a letter by Hwa, Speisbach, and Teper¹⁵ appeared, in which a fit similar to ours is presented for the inclusive $pp \rightarrow \pi^0 X$ CERN ISR data. Unlike the present paper, which attempts to fit all the available data in a purely phenomenological way, these authors obtain a zero-parameter fit to the $pp \rightarrow \pi^0 X$ data by

modifying the naive BBK cross section to incorporate the Chanowitz-Drell⁸ quark form factors. The difference between their result, which corresponds to $B=50 \text{ GeV}^2$, and ours arises from the fact that our value of B is chosen to give the best overall fit to a substantially larger body of experimental data.

II. CROSS-SECTION CALCULATION

We present in this section the details of the EG model for the inclusive production of hadrons with large transverse momenta. Our parton-model treatment is similar to those given earlier by various authors.^{6,7,9} Throughout this paper we will assume that hadrons are described by the conventional 3-quark model in which the quark-partons are designated by u , d , and s , and we will use the terms quark and parton interchangeably. As in the elementary BBK model we assume that the production mechanism proceeds via the following steps, as shown in Fig. 1: The initial hadrons fragment into quarks, which then scatter from each other via some as yet unspecified mechanism. The quarks then "decay" into the final hadrons, one of which is the observed particle. The inclusive cross section is then obtained by summing or integrating over all possible quark-quark scattering processes which can lead from a given initial state to the same final state. Referring to the notation of Fig. 1 we introduce the parton variables

$$\begin{aligned}\hat{x}_1 &= -\frac{(p_i - p_k)^2}{(p_i + p_j)^2} = -\frac{\hat{u}}{\hat{s}}, \\ \hat{x}_2 &= -\frac{(p_i - p_l)^2}{(p_i + p_j)^2} = -\frac{\hat{t}}{\hat{s}},\end{aligned}\quad (2.1)$$

$$\begin{aligned}E_c \frac{d\sigma}{d^3p_c} &= \frac{1}{\pi s} \frac{d\sigma}{dx_1 dx_2} \\ &= \frac{1}{\pi s} \sum_{ij} \int \int u_i(x_i) u_j \left(\frac{x_2 x_i}{x_i x - x_1} \right) [f(x_1, x_2; x_i, x) G_{i/c}(x) + f'(x_1, x_2; x_i, x) G_{j/c}(x) \\ &\quad + \delta_{ij} G_{i/c}(x) f''(x_1, x_2; x_i, x)] \frac{dx_i dx}{x^2 (x_i x - x_1)}.\end{aligned}\quad (2.6)$$

In Eq. (2.6) $u_i(z)$ is the probability that an incident proton contains a parton of type i ($i=u, d, s, \bar{u}, \bar{d}, \bar{s}$ for the usual quark model) which carries a fraction z of the initial proton's 4-momentum. Similarly $G_{i/c}(x)/x$ is the probability that parton i will "decay" into hadron c , with c carrying a fraction x of the initial parton's 4-momentum. (We assume, of course, that the energy is sufficiently high that both the hadrons and the partons can be taken as massless.) The term proportional to f' is included to take account of the fact that the observed hadron

and the corresponding variables for the observed process,

$$\begin{aligned}x_1 &= -\frac{(p_b - p_c)^2}{(p_a + p_b)^2} = -\frac{u}{s}, \\ x_2 &= -\frac{(p_a - p_c)^2}{(p_a + p_b)^2} = -\frac{t}{s}.\end{aligned}\quad (2.2)$$

In terms of these variables the differential cross section for a parton-parton scattering such as $u(p_i) + d(p_j) \rightarrow u(p_l) + d(p_k)$ is given by

$$\begin{aligned}d\hat{\sigma} &= \tilde{f}(x_1, x_2; \hat{x}_1, \hat{x}_2) \delta(\hat{x}_1 + \hat{x}_2 - 1) d\hat{x}_1 d\hat{x}_2 \\ &= f(x_1, x_2; \hat{x}_1) d\hat{x}_1,\end{aligned}\quad (2.3)$$

where the functions \tilde{f} and f depend on the detailed dynamics of the scattering process. It is convenient to introduce a second cross section $d\hat{\sigma}'$ defined by

$$d\hat{\sigma}'(p_l, p_k) = d\hat{\sigma}(p_k, p_l) = f'(x_1, x_2; \hat{x}_1) d\hat{x}_1. \quad (2.4)$$

$d\hat{\sigma}$ and $d\hat{\sigma}'$ thus represent the parton-parton differential cross sections in the \hat{t} and \hat{u} channels, respectively. For the scattering of identical partons we have

$$d\hat{\sigma}^{\text{ident}} = d\hat{\sigma} + d\hat{\sigma}' + f''(x_1, x_2; \hat{x}_1) d\hat{x}_1, \quad (2.5)$$

where f'' arises from the interference between the \hat{t} -channel and \hat{u} -channel contributions. The use of Eqs. (2.3)–(2.5) will be demonstrated below.

Given the parton-parton differential cross sections, the invariant cross section for the production of particle c can be written as follows:

can come from either of the scattered quarks, while f'' represents an additional contribution which arises when the scattering quarks are identical.

In evaluating the invariant cross section using Eq. (2.6) we have assumed that the scattered quark appears as a valence quark of the observed particle. Thus, for example, in calculating the cross section for $pp \rightarrow \pi^+ X$, only the u and \bar{d} contributions to \sum_{ij} are included. We have also ignored contributions from quark-antiquark ($q\bar{q}$) annihilation

processes, such as $q\bar{q} \rightarrow \text{gluon} \rightarrow q\bar{q}$, since these necessarily arise from the parton sea whose contribution is small in the models we consider.¹⁶ For the distribution functions $u_i(z)$ we have used the modified Kutl-Weisskopf¹⁷ (MKW) functions of McElhaney and Tuan,¹⁸ which are extracted from the deep-inelastic electroproduction data. For the distribution functions $G_{i/c}$ we have taken the functions defined by BBK,⁶ and have assumed that the same functional form characterizes the "decay" of a parton into both strange and nonstrange mesons. More specifically

$$G_{i/c}(z) = \kappa_{i/c} [2(1-z)] \quad (\text{meson production}), \quad (2.7a)$$

$$G_{i/c}(z) = \kappa_{i/c} [5.78\nu W_2(z)] \quad (\text{baryon production}), \quad (2.7b)$$

where $\nu W_2(z)$ is the usual deep-inelastic electroproduction structure function. The $\kappa_{i/c}$ are constants which represent the fraction of the time that parton i decays into hadron c . As defined above, they satisfy the normalization condition

$$\sum_c \kappa_{i/c} = 1, \quad (2.8)$$

which follows from energy conservation in the parton decay.⁶

Having specified the parton distribution functions

in Eq. (2.6) we turn to a discussion of the functions f , f' , and f'' , which describe the dynamics of the parton-parton interaction. The starting point for the EG model is the differential cross section in the center of momentum (c.m.) for the scattering of two identical massless spin- $\frac{1}{2}$ partons, via the exchange of a massless vector gluon:

$$\frac{d\hat{\sigma}}{d\hat{\Omega}} = \frac{\alpha_s^2}{2\hat{s}} \left[\frac{1 + \cos^4(\hat{\theta}/2)}{\sin^4(\hat{\theta}/2)} + \frac{1 + \sin^4(\hat{\theta}/2)}{\cos^4(\hat{\theta}/2)} + \frac{2}{\sin^2(\hat{\theta}/2) \cos^2(\hat{\theta}/2)} \right]. \quad (2.9)$$

In Eq. (2.9) $\alpha_s = g^2/4\pi$, where g is the strong parton-parton-gluon coupling constant, and $\hat{\theta}$ is the c.m. scattering angle. Equation (2.9) is, of course, the familiar expression for Møller scattering,¹⁹ with α_s replacing the usual fine-structure constant α . The differential cross section for the scattering of nonidentical partons is then obtained from the expression in Eq. (2.9) by dropping the second and third terms in the square brackets. The EG model is obtained from (2.9) by multiplying each parton-parton-gluon vertex by the function

$$F(\xi) = (1 - \xi/B)^{-1}, \quad (2.10)$$

where $\xi = \hat{t}$ or \hat{u} is the appropriate momentum transfer at the parton-parton-gluon vertex, and B is a constant. In the EG model, Eq. (2.9) is thus replaced by

$$\frac{d\hat{\sigma}^{\text{EG}}}{d\hat{\Omega}} = \frac{\alpha_s^2}{2\hat{s}} \left[\frac{1 + \cos^4(\hat{\theta}/2)}{\sin^4(\hat{\theta}/2)} F^4(\hat{t}) + \frac{1 + \sin^4(\hat{\theta}/2)}{\cos^4(\hat{\theta}/2)} F^4(\hat{u}) + \frac{2}{\sin^2(\hat{\theta}/2) \cos^2(\hat{\theta}/2)} F^2(\hat{t}) F^2(\hat{u}) \right]. \quad (2.11)$$

Using the kinematic relations,

$$\hat{x}_1 = \frac{1}{2}(1 + \cos\hat{\theta}) = x_1/x_i x, \quad (2.12a)$$

$$\hat{x}_2 = \frac{1}{2}(1 - \cos\hat{\theta}) = x_2/x_j x, \quad (2.12b)$$

$$x_j = x_i x_2 / (x_i x - x_1), \quad (2.12c)$$

it is a straightforward matter to express Eq. (2.11) in the form of Eq. (2.5), and to thereby extract the functions f , f' , and f'' . We find

$$f(x_1, x_2; x_i, x) = \frac{2\pi\alpha_s^2}{s} \frac{(x_i^2 x^2 + x_1^2)}{x_i^2 x_2 (x_i x - x_1)} \frac{B^4 x^4}{(Bx + x_i x_2 s)^4}, \quad (2.13a)$$

$$f'(x_1, x_2; x_i, x) = \frac{2\pi\alpha_s^2}{s} \frac{(x_i x - x_1)(2x_i^2 x^2 - 2x_i x x_1 + x_1^2)}{x_i^2 x_1^2 x_2} \frac{B^4 x^4 (x_i x - x_1)^4}{[Bx(x_i x - x_1) + x_1 x_2 x_i s]^4}, \quad (2.13b)$$

$$f''(x_1, x_2; x_i, x) = \frac{2\pi\alpha_s^2}{s} \frac{2x^2}{x_1 x_2} \frac{B^4 x^4 (x_i x - x_1)^2}{(Bx + x_2 x_i s)^2 [Bx(x_i x - x_1) + x_1 x_2 x_i s]^2} \quad (2.13c)$$

To illustrate the use of Eqs. (2.6) and (2.13) under the assumptions we have made, we quote the expression for the invariant differential cross section for $p\bar{p} \rightarrow \pi^+ X$. Recalling that π^+ is composed of u and \bar{d} valence quarks, we have

$$\begin{aligned}
E_{\pi^+} \frac{d\sigma}{d^3p_{\pi^+}} &= \frac{1}{\pi s} \int_{x_1/(1-x_2)}^1 dx_i \\
&\times \int_{x_2+x_1/x_i}^1 dx \left\{ [u_u(x_i)\kappa_{u/\pi^+} + u_{\bar{d}}(x_i)\kappa_{\bar{d}/\pi^+}] \left[\sum_j u_j \left(\frac{x_i x_2}{x_i x - x_1} \right) \right] f(x_1, x_2; x_i, x) \right. \\
&+ \left[\sum_i u_i(x_i) \right] \left[u_u \left(\frac{x_i x_2}{x_i x - x_1} \right) \kappa_{u/\pi^+} + u_{\bar{d}} \left(\frac{x_i x_2}{x_i x - x_1} \right) \kappa_{\bar{d}/\pi^+} \right] f'(x_1, x_2; x_i, x) \\
&+ \left. \left[u_u(x_i) u_u \left(\frac{x_i x_2}{x_i x - x_1} \right) \kappa_{u/\pi^+} + u_{\bar{d}}(x_i) u_{\bar{d}} \left(\frac{x_i x_2}{x_i x - x_1} \right) \kappa_{\bar{d}/\pi^+} \right] f''(x_1, x_2; x_i, x) \right\} \frac{2(1-x)}{x^2(x_i x - x_1)}.
\end{aligned} \tag{2.14}$$

Note that Eq. (2.14) is of the form

$$\begin{aligned}
E_{\pi^+} \frac{d\sigma}{d^3p_{\pi^+}} &= \alpha_s^2 (\kappa_{u/\pi^+} \langle u \rangle + \kappa_{\bar{d}/\pi^+} \langle \bar{d} \rangle) \\
&= \alpha_s^2 \kappa_{u/\pi^+} \left[1 + \left(\frac{\kappa_{\bar{d}/\pi^+}}{\kappa_{u/\pi^+}} - 1 \right) \frac{\langle \bar{d} \rangle}{\langle u \rangle + \langle \bar{d} \rangle} \right] (\langle u \rangle + \langle \bar{d} \rangle) \\
&\equiv \alpha_s^2 \kappa_{\pi^+} (\langle u \rangle + \langle \bar{d} \rangle),
\end{aligned} \tag{2.15}$$

where α_s^2 has been factored out of the f 's, and where $\langle u \rangle$ and $\langle \bar{d} \rangle$ denote the integrals containing u_u and $u_{\bar{d}}$, respectively in Eq. (2.14). We see from Eq. (2.15) that if $\kappa_{u/\pi^+} \cong \kappa_{\bar{d}/\pi^+}$ then the normalization $\alpha_s^2 \kappa_{\pi^+}$ obtained from the fit to the π^+ data is just a measure of $\alpha_s^2 \kappa_{u/\pi^+}$. Moreover, since the \bar{d} quark occurs only in the parton sea, we expect that $\langle \bar{d} \rangle \ll \langle u \rangle$, and hence the second term in square brackets in (2.15) should be small²⁰ even if $\kappa_{u/\pi^+} \neq \kappa_{\bar{d}/\pi^+}$. We are thus safe in using $E_{\pi^+} d\sigma/d^3p_{\pi^+}$ as a measure of $\alpha_s^2 \kappa_{u/\pi^+}$, and similarly for the other κ 's, where the production of π^0 , π^- , K^+ , K^- , p , and \bar{p} determine $\alpha_s^2 \kappa_{d/\pi^0} = \alpha_s^2 \kappa_{u/\pi^0}$, $\alpha_s^2 \kappa_{d/\pi^-} = \alpha_s^2 \kappa_{u/\pi^-}$, $\alpha_s^2 \kappa_{u/K^+} = \frac{1}{2} \alpha_s^2 (\kappa_{u/K^-} + \kappa_{s/K^-})$, $\alpha_s^2 \kappa_{u/p} = \alpha_s^2 \kappa_{d/p}$, and $\frac{1}{2} \alpha_s^2 (\kappa_{u/\bar{p}} + \kappa_{\bar{d}/\bar{p}})$, respectively. The consistency of the EG model can then be tested by checking that the values of the constants so obtained are the same irrespective of which data are used to extract them. In addition to the constants $\alpha_s^2 \kappa_{u/\pi^+}$, etc., one can also determine the ratios $\kappa_{u/\pi^+}/\kappa_{\bar{d}/\pi^+}$ using charge conjugation and thereby determine whether their ratio is indeed unity. We will return to discuss these constants in greater detail below.

In calculating the p -nucleon cross sections which correspond to those extracted from p -nucleus scattering at Fermilab,¹⁴ we have averaged the results for $pp \rightarrow cX$ and $pn \rightarrow cX$, where $c = \pi^\pm, \pi^0, p, \dots$, etc. The quark distribution functions for the neutron were obtained from those for the proton by using pn isospin invariance.²¹ Although this procedure is by no means rigorous, it is not expected to introduce any significant distortions into the comparison of theory and experiment.

We conclude this section by enumerating the pa-

rameters which characterize the EG model. The dependence of $E_c d\sigma/d^3p_c$ on s and x_1 , for $c = p, \bar{p}, \pi^\pm, \pi^0$, and K^\pm , is determined by a *single universal constant* B , with the best fit being given by $B = 18$ GeV². There is, in addition, a single normalization constant for each c , namely $\alpha_s^2 \kappa_{\pi^+}, \dots$, etc., which fixes the overall scale. Using the sum rule of Eq. (2.8) and the values of the normalization constants $\alpha_s^2 \kappa_{\pi^+}, \dots$, we can solve for α_s . The result, which is derived in Sec. III below, is

$$2.8 \lesssim \alpha_s \lesssim 3.5. \tag{2.16}$$

III. COMPARISON TO EXPERIMENT

Figures 2-16 show the results of our calculations for the values of s and x_1 which have been measured experimentally. The data for π^0 production are taken from the CERN-Columbia-Rockefeller CERN-ISR results of Refs. 10 and 11. The data on charged-particle production come from the British-Scandinavian (BS) collaboration^{12,13} at the CERN-ISR, and from the Chicago-Princeton (CP) collaboration¹⁴ at Fermilab. To check the consistency of the EG model we have evaluated the normalization constants $\alpha_s^2 \kappa_{u/\pi^+}, \dots$, etc., separately for each value of s and θ , and the results are shown in Figs. 17 and 18. We see from these figures that the various determinations of these constants²² give results which are in generally good agreement with one another. It is interesting to note that, with the exception of the baryon data from the Chicago-Princeton collaboration, there are no *systematic* variations of the normalization constants with s or θ . This suggests that the EG model is not overlooking a significant contribution to the s or θ dependence of $E_c d\sigma/d^3p_c$.

Another check on the consistency of the model is obtained by studying the sensitivity of the results to the parameter B . If B is changed from 18 GeV² to 20 GeV² the overall quality of the fit is not greatly affected, but the values of all the normalization constants $\alpha_s^2 \kappa_{u/\pi^+}, \dots$, are decreased by $\sim 15\%$. The ratios of the normalization constants, however,

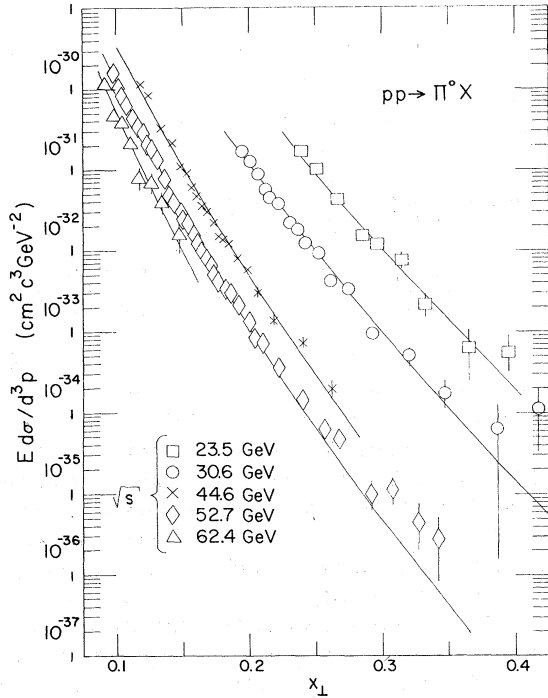


FIG. 2. Invariant cross section versus $x_1 = 2p_1/\sqrt{s}$ for $pp \rightarrow \pi^0 X$ at ISR laboratory scattering angle $\theta = 90^\circ$. The experimental data are from Ref. 10, and the solid curves are those obtained from the EG model.

remain unchanged, which confirms the interpretation we have given them as fundamental parameters of the theory. Evidently these ratios should also be expected to be independent of s . That this is indeed the case is shown in Fig. 19, along with the average values of the various ratios. It is seen that the various determinations of the ratios of the normalization constants are in very good agreement with one another. Since these ratios are independent of B and, more importantly, of the normalizations of the experimentally determined cross sections, they are the best gauge of the consistency of the EG model, and hence the agreement among the various determinations of these ratios lends support to the model.

$$R_{\pi^+} = \frac{[1 - \langle \bar{d} \rangle_{\pi^+} / \langle \langle u \rangle_{\pi^+} + \langle \bar{d} \rangle_{\pi^+}] (\kappa_{\pi^-} / \kappa_{\pi^+}) - [\langle \bar{u} \rangle_{\pi^-} / \langle \langle \bar{d} \rangle_{\pi^-} + \langle \bar{u} \rangle_{\pi^-}]}{[1 - \langle \bar{u} \rangle_{\pi^-} / \langle \langle \bar{d} \rangle_{\pi^-} + \langle \bar{u} \rangle_{\pi^-}] - [\langle \bar{d} \rangle_{\pi^+} / \langle \langle u \rangle_{\pi^+} + \langle \bar{d} \rangle_{\pi^+}] (\kappa_{\pi^-} / \kappa_{\pi^+})}. \quad (3.1)$$

In Eq. (3.1) $\langle u \rangle_{\pi^+}$ denotes the quantity $\langle u \rangle$ appearing in the expression for $E_\pi d\sigma/d^3p_\pi$ in Eq. (2.15), and analogously for $\langle \bar{u} \rangle_{\pi^-}$, etc. For the MKW¹⁷ distribution functions that we have used

$$\frac{\langle \bar{d} \rangle_{\pi^+}}{\langle u \rangle_{\pi^+} + \langle \bar{d} \rangle_{\pi^+}} \cong 0.08, \quad \frac{\langle \bar{u} \rangle_{\pi^-}}{\langle \bar{d} \rangle_{\pi^-} + \langle \bar{u} \rangle_{\pi^-}} \cong 0.16, \quad (3.2)$$

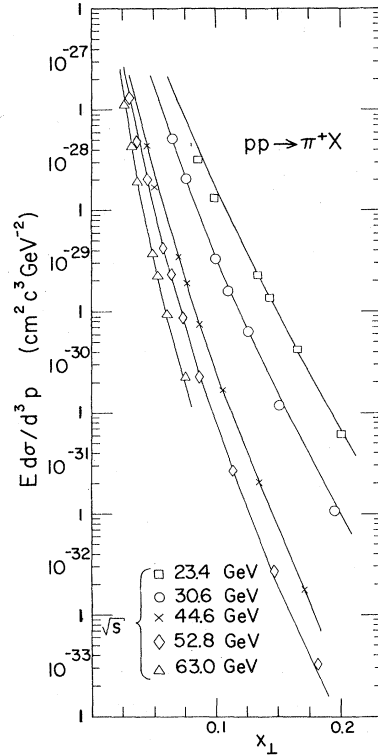


FIG. 3. Invariant cross section versus $x_1 = 2p_1/\sqrt{s}$ for $pp \rightarrow \pi^+ X$ at ISR laboratory scattering angle $\theta = 89^\circ$. The experimental data for Figs. 3–10 are from Ref. 12, and the solid curves are those obtained from the EG model.

By varying the parameter B we can also compare our results to those of Hwa *et al.*¹⁵ for the π^0 data of Ref. 10. We find that their value $B = 50 \text{ GeV}^2$ does indeed give an acceptable fit to the π^0 data, but is not as good in describing all the data as is our value $B = 18 \text{ GeV}^2$.

From Fig. 19, and the assumption that the parton functions $G(x)$ are charge-conjugation invariant (so that $\kappa_{d/\pi^-} = \kappa_{\bar{d}/\pi^+}$), we find that $\kappa_{\bar{d}/\pi^+} / \kappa_{u/\pi^+} \cong 1.53$. Using Eq. (2.15), along with the equivalent π^- equation and charge-conjugation invariance, the ratio $R_{\pi^+} = \kappa_{\bar{d}/\pi^+} / \kappa_{u/\pi^+}$ is related to the value of $\kappa_{\pi^-} / \kappa_{\pi^+}$ emerging from our fit as follows:

and hence $R_{\pi^+} \cong 1.7$. In a similar manner we obtain $R_{K^+} = \kappa_{\bar{s}/K^+} / \kappa_{u/K^+} \cong 13$ and $R_{\pi^-} = \kappa_{u/\pi^-} / \kappa_{d/\pi^-} \cong 5.0$.

The above results for R_{π^+} and R_{K^+} are in agreement with the conjecture, for which there is some experimental evidence,²³ that the strange quark in the kaon carries a much larger fraction of the kaon momentum than does the nonstrange quark. This

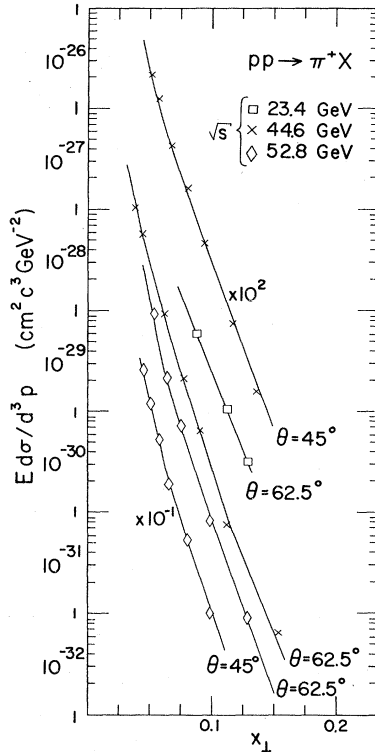


FIG. 4. Invariant cross section versus x_{\perp} for $pp \rightarrow \pi^+ X$. θ denotes the ISR laboratory scattering angle. The uppermost curve displays the value of the invariant cross section at $\sqrt{s} = 44.6$ GeV and $\theta = 45^\circ$ multiplied by 100, and the lowest curve displays the $\sqrt{s} = 52.8$ GeV and $\theta = 45^\circ$ values divided by 10. Data are from Ref. 12.

conjecture is motivated by the assumption that the strange quark is heavier than the nonstrange quark, owing to SU(3)-symmetry breaking, and thus suggests that the analogous effect for the u and \bar{d} quarks in the pion, where SU(2)-breaking effects are small, should be much less pronounced. The value of the ratio $R_{\pi/K}$ supports our general expectation that a nonstrange quark should evolve more readily into a pion than into a kaon. This notion is also borne out for baryons by recently published data on inclusive Λ and $\bar{\Lambda}$ production at large p_{\perp} .²⁴ This experiment indicates that (at 90° in the c.m.) the p and Λ inclusive differential cross sections have roughly the same shape, as do the \bar{p} and $\bar{\Lambda}$ cross sections, but that Λ and $\bar{\Lambda}$ production is roughly four times smaller than p and \bar{p} production.

The ratio $\kappa_p/\kappa_{\bar{p}}$ shown in Fig. 19 does not appear to support our use of charge-conjugation invariance, which would require that $\kappa_p/\kappa_{\bar{p}} \cong 1.0$. Here, however, the situation is complicated by the fact that the scattering of the valence quark of the incident protons into the sea of the observed particles is likely to be much more important for baryons than for mesons, because of the difference in

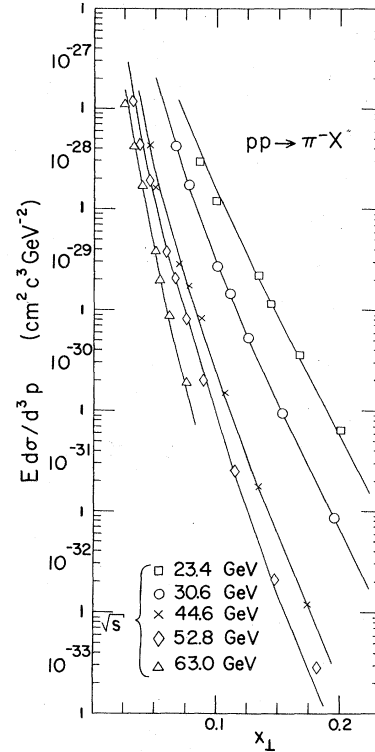


FIG. 5. Invariant cross section versus x_{\perp} for $pp \rightarrow \pi^- X$ at $\theta = 89^\circ$. Data are from Ref. 12.

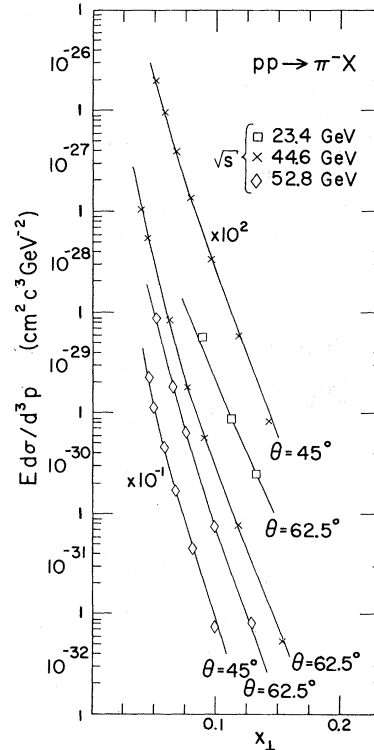


FIG. 6. Invariant cross section versus x_{\perp} for $pp \rightarrow \pi^- X$. The notation is the same as that of Fig. 4, and the data are from Ref. 12.

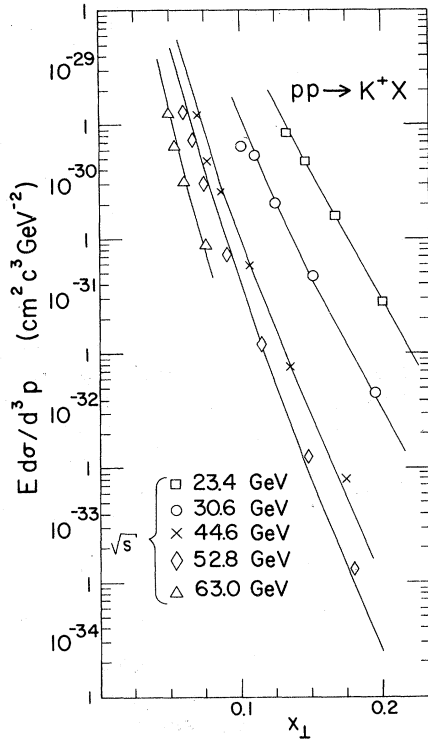


FIG. 7. Invariant cross section versus x_1 for $pp \rightarrow K^+X$ at $\theta=89^\circ$. Data are from Ref. 12.

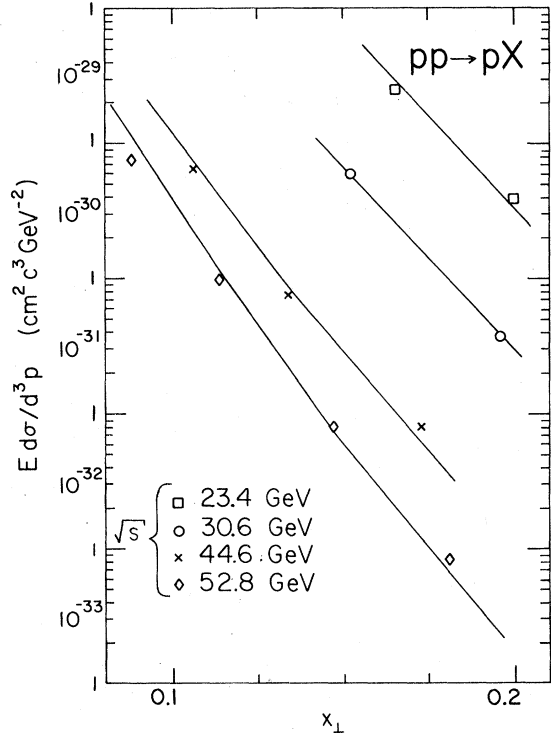


FIG. 9. Invariant cross section versus x_1 for $pp \rightarrow pX$ at $\theta=89^\circ$. Data are from Ref. 12.

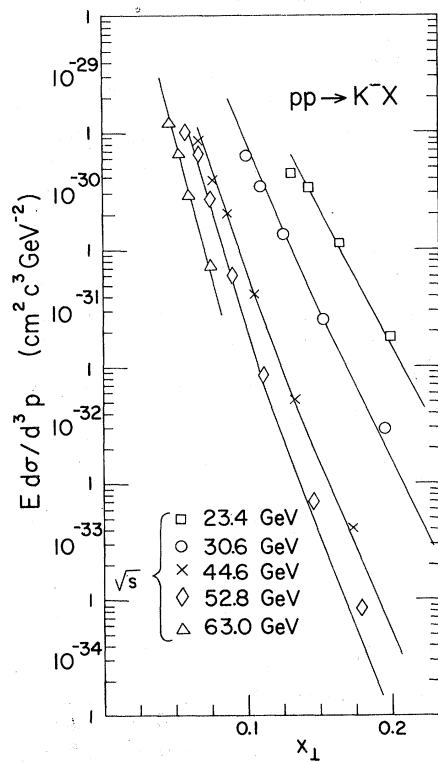


FIG. 8. Invariant cross section versus x_1 for $pp \rightarrow K^-X$ at $\theta=89^\circ$. Data are from Ref. 12.

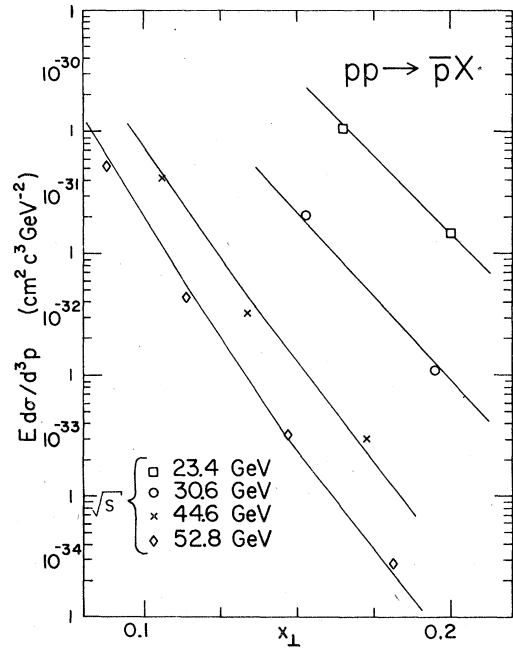


FIG. 10. Invariant cross section versus x_1 for $pp \rightarrow \bar{p}X$ at $\theta=89^\circ$. Data are from Ref. 12.

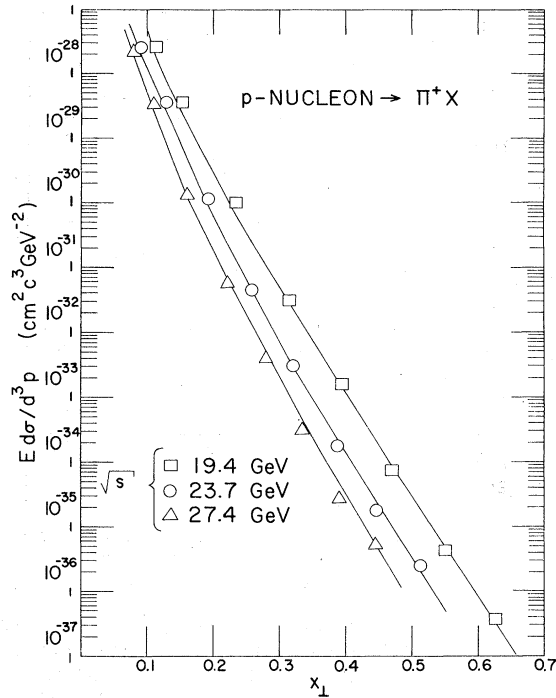


FIG. 11. Invariant cross section versus x_1 for p -nucleon $\rightarrow \pi^+ X$. The solid curves are those obtained from the EG model for $\sqrt{s} = 19.4$ GeV and center-of-momentum scattering angle $\theta = 77^\circ$; $\sqrt{s} = 23.7$ GeV, $\theta = 88.5^\circ$; and $\sqrt{s} = 27.4$ GeV, $\theta = 96.7^\circ$. The experimental data are from Ref. 14.

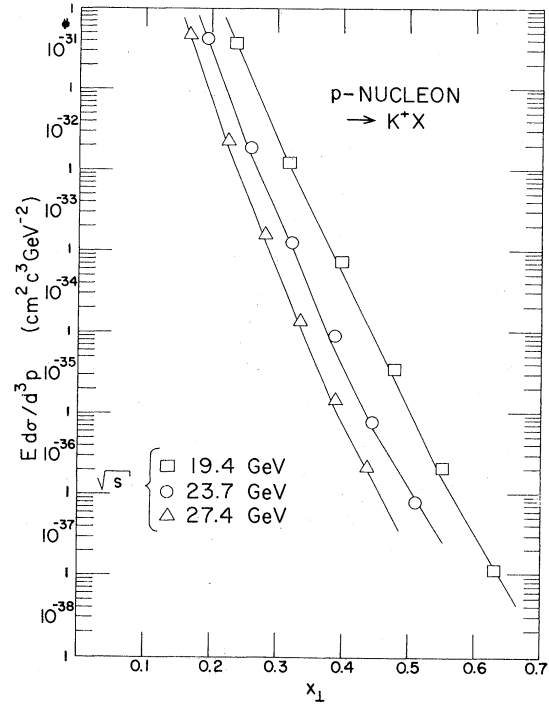


FIG. 13. Invariant cross section versus x_1 for p -nucleon $\rightarrow K^+ X$. Data are from Ref. 14.

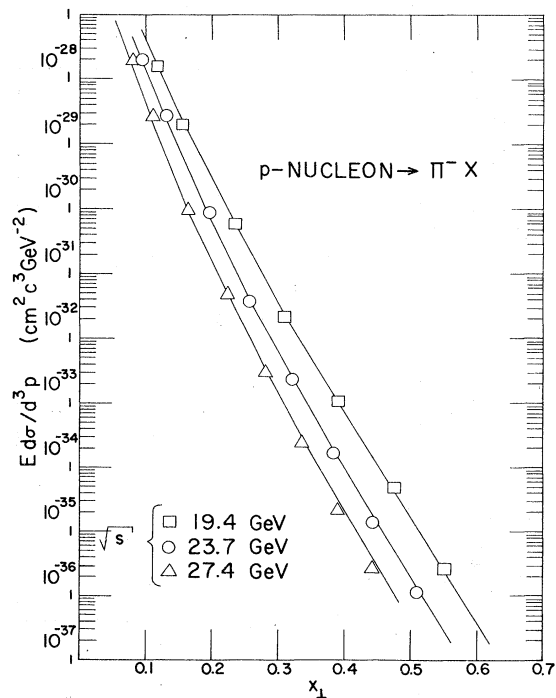


FIG. 12. Invariant cross section versus x_1 for p -nucleon $\rightarrow \pi^- X$. Data are from Ref. 14.

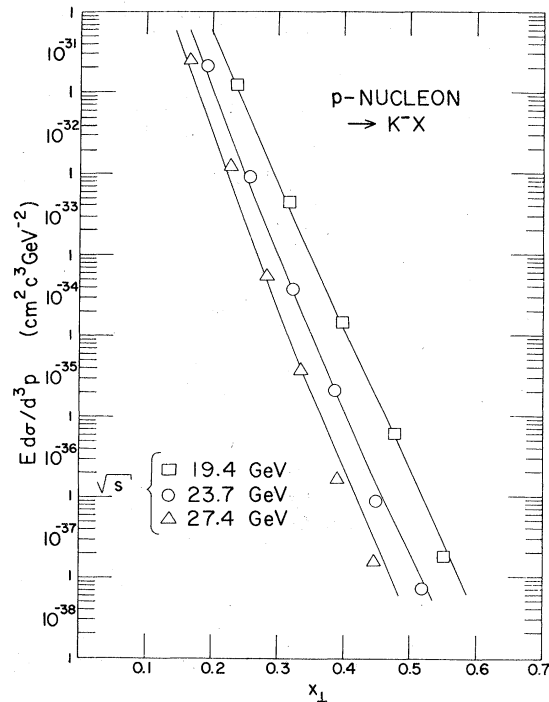


FIG. 14. Invariant cross section versus x_1 for p -nucleon $\rightarrow K^- X$. Data are from Ref. 14.

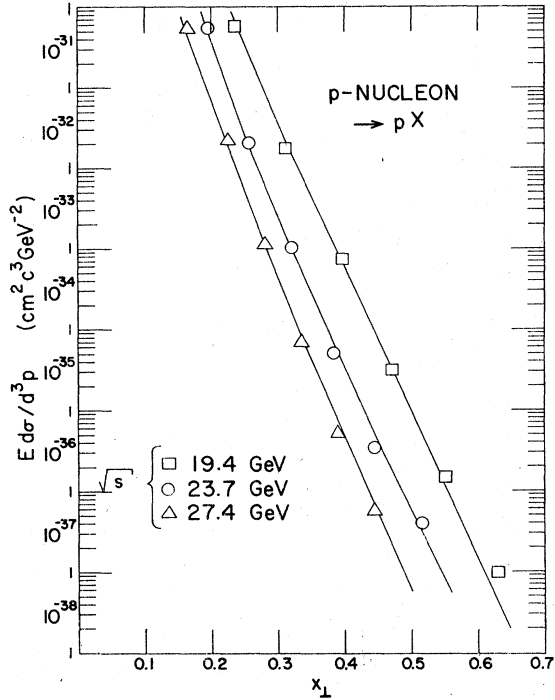


FIG. 15. Invariant cross section versus x_{\perp} for p -nucleon $\rightarrow pX$. Data are from Ref. 14.

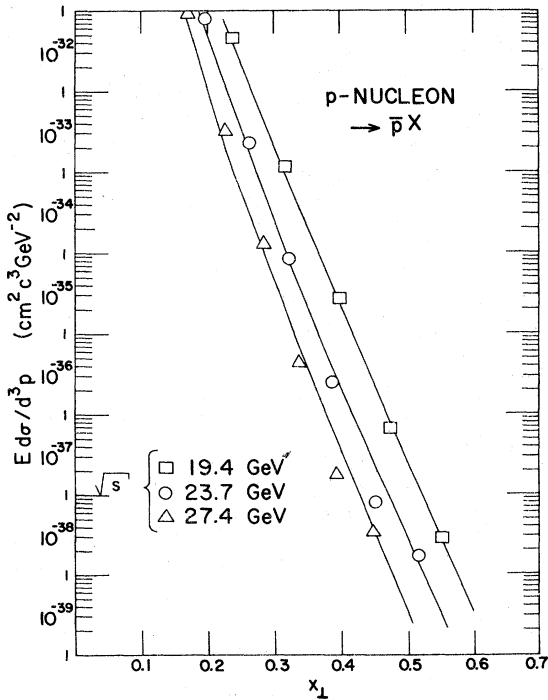


FIG. 16. Invariant cross section versus x_{\perp} for p -nucleon $\rightarrow \bar{p}X$. Data are from Ref. 14.

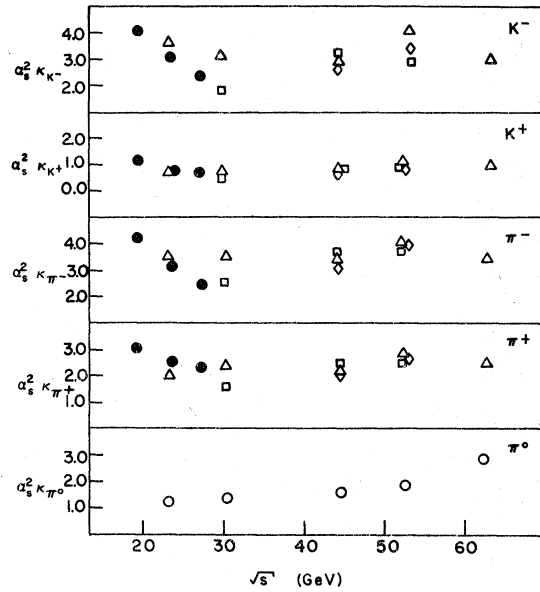


FIG. 17. Meson normalization constants for the curves of Figs. 2-16. The closed circles are calculated for the data of the CP collaboration (Ref. 14); the triangles, squares, and diamonds are calculated for the data of the BS collaboration (Ref. 13) at ISR laboratory scattering angles $\theta=89^\circ, 62.5^\circ,$ and 45° , respectively; the open circles are calculated for the data of the CCR collaboration (Ref. 10). The π^0 values have been corrected for the more recent experimental normalization of Ref. 11.

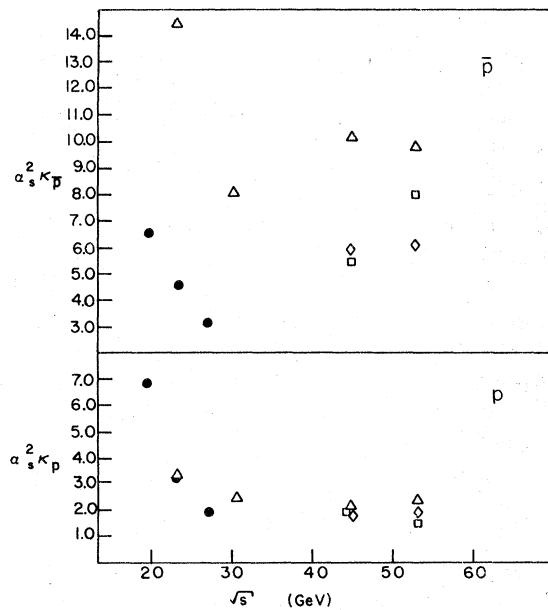


FIG. 18. Baryon normalization constants for the curves of Figs. 2-16. For an explanation of the symbols see Fig. 17.

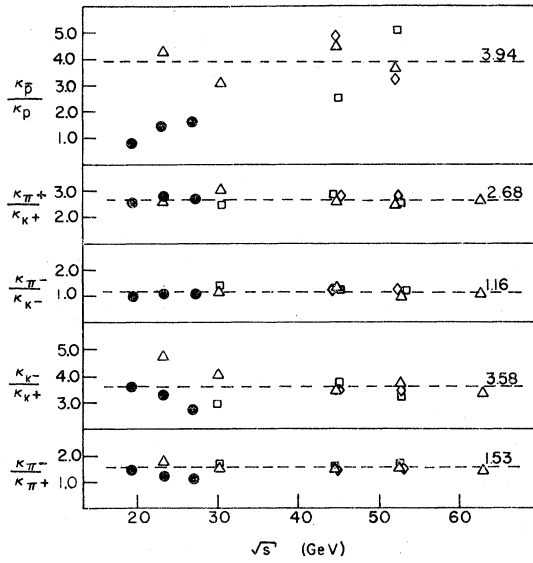


FIG. 19. Ratios of the normalization constants given in Figs. 17 and 18, along with their average values, shown by the dotted lines. For an explanation of the symbols see Fig. 17.

the respective expressions for $G(z)$ in Eq. (2.7). For example, inclusion of such a contribution with $G(z) \propto (1-z)^{3.5}$ and $\kappa_{sea} = \kappa_{d/p}$ brings the ratio $\kappa_p/\kappa_{\bar{p}}$ close to the desired value. A similar term added to the expression for the K^- cross section changes the overall K^- normalization by only $\sim 5\%$, so that the meson results are not significantly affected. We also note that our assumption that the hadrons are effectively massless is likely to be much less justified for baryons than for mesons for the values of p_\perp in the present experiments, and hence the baryon results are somewhat more uncertain than those for mesons.

An approximate value for α_s can be obtained by using the values for the ratios of the κ 's in conjunction with the sum rule of Eq. (2.8). To use Eq. (2.8) we assume that the u quark decays principally into π^+ , π^0 , K^+ , p , and n , and that the d quark decays principally into π^- , π^0 , K^0 , \bar{p} , and n . Taking the values of the ratios of the κ 's found from the EG-model fit along with the additional assumptions that $\kappa_{u/p} \cong 2\kappa_{u/n}$ and $\kappa_{u/\pi^+}/\kappa_{u/K^+} \cong \kappa_{d/\pi^-}/\kappa_{d/K^0}$, we find

$$0.2 \lesssim \kappa_{u/\pi^+} \lesssim 0.3$$

and (3.3)

$$0.3 \lesssim \kappa_{d/\pi^-} \lesssim 0.4.$$

Combining these with the average values $\langle \alpha_s^2 \kappa_{u/\pi^+} \rangle \cong 2.4$ and $\langle \alpha_s^2 \kappa_{d/\pi^-} \rangle \cong 3.5$ from Fig. 17 gives

$$2.8 \lesssim \alpha_s \lesssim 3.5. \quad (3.4)$$

We turn next to consider the x_\perp dependence (over the range of ISR energies) of the exponent n defined by

$$E \frac{d\sigma}{d^3p} = (p_\perp)^{-n} g_n(x_\perp) = (\sqrt{s})^{-n} h_n(x_\perp). \quad (3.5)$$

In the naive parton model, in which both the parton and gluon are massless, $g_n(x_\perp)$ and $h_n(x_\perp)$ would be dimensionless functions of the variable x_\perp . It then follows from naive dimensional arguments that n must equal 4, a prediction which is not borne out by experiment. The introduction of a mass parameter such as B makes it possible for $g_n(x_\perp)$ and $h_n(x_\perp)$ to have dimensions, in which case n can assume values other than 4.²⁵ The variation of n with x_\perp at ISR energies in the EG model is shown in Fig. 20 for π^+ and p production. The qualitative feature of the model, that the baryon cross sections fall more rapidly with increasing s at fixed x_\perp than do the meson cross sections, is seen experimentally.^{13,14} Quantitatively, the values of $n(x_\perp)$ at fixed s agree in general with those obtained for $x_\perp < 0.3$ by both the BS¹³ and CP¹⁴ groups. We note from Eqs. (2.13) and (2.14) that the largest value of n that can arise in the EG model is $n=12$, and hence this model does not account for the values $n > 12$ which are observed at Fermilab¹⁴ in proton production at $x_\perp > 0.3$. However, the x_\perp dependence of this data at constant s is adequately described by the EG model for large x_\perp . It is possible that the discrepancy between the prediction of the EG model and experiment could arise from the procedure for extracting the p -nucleon cross sections from the p -nucleus data. This possibility could be explored

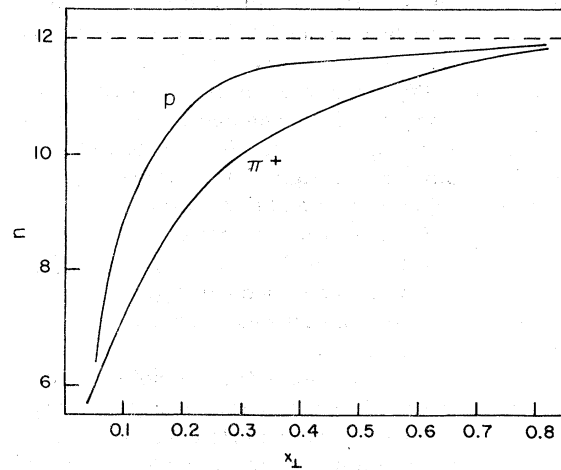


FIG. 20. EG-model values of n versus x_\perp for p and π^+ extracted for the energy range $800 \text{ GeV}^2 \leq s \leq 4000 \text{ GeV}^2$. This corresponds to the parametrization of the cross section in the form $E_c d\sigma/d^3p_c = (p_\perp)^{-n} g_n(x_\perp)$.

by measuring the pp cross section directly for $x_1 > 0.3$, or by studying the dependence of the cross section on nucleon number at various energies in p -nucleus scattering.

$$E \frac{d\sigma^{\text{jet}}}{d^3p} = \frac{1}{\pi s} \sum_{ij} \int u_i(x_i) u_j \left(\frac{x_2 x_i}{x_i - x_1} \right) [f(x_1, x_2; x_i, x=1) + f'(x_1, x_2; x_i, x=1) + \delta_{ij} f''(x_1, x_2; x_i, x=1)] \frac{dx_i}{x_i - x_1}. \quad (3.6)$$

The jet cross section for several values of s is shown in Fig. 21. Since the parton decay functions $G_{i/c}(z)$ do not appear in Eq. (3.6), the jet cross section does not depend on the unknown constants $\kappa_{i/c}$. The jet cross section is thus directly proportional to the parton-parton-gluon coupling constant α_s (which is buried in the functions f , f' , and f'') and so can be used to determine α_s directly. If jet cross sections of the general form predicted here are observed, it may be possible to use the experimental results to improve upon the quark-quark cross section and, in turn, to obtain more detailed information about the parton decay functions $G_{i/c}(z)$.

IV. CONCLUSIONS

We have shown that a modification of the quark-quark scattering model of Refs. 6 and 7 leads to a simple model of inclusive meson and baryon production in good agreement with the data. The effective-gluon (EG) model so obtained is characterized by a single universal constant $B = 18 \text{ GeV}^2$, which accounts for the s , x_1 , and θ dependence of all the measured inclusive differential cross sections. The curves of Figs. 2–16, which were generated for the case where all κ 's involved in the production of a single particle are equal, require an additional seven normalization constants to fix the overall scale. The resulting fit is good to roughly 5–20% per data point over 10 orders of magnitude for $E d\sigma/d^3p$. The one exception comes for the K^- curves, where the fit is good to ~40% per data point. More significantly there are no systematic discrepancies between the data and the EG model. We note that the best fit was obtained with the functional form for $F(\xi)$ as given in Eq. (2.10), with other forms (such as exponential and dipole) unable to simultaneously reproduce all features of the data.

The EG model was motivated, as noted previously, by our desire to construct an analytic expression for the strong parton-parton scattering amplitude which could be combined coherently with the weak amplitude of Ref. 1. We thus conclude by giving the complete quark-quark scattering amplitude τ obtained by combining the EG amplitude and the weak model of Ref. 1, assuming maximal con-

The EG model can also be used to analyze jet production in high-energy collisions.^{26,27} Using the same notation as in Eq. (2.6) the inclusive jet cross section is given by

structive interference for illustrative purposes:

$$\begin{aligned} \tau &= \tau_s + \tau_w \\ &= 4\pi \alpha_s \hat{t}^{-1} (1 - \hat{t}/B)^{-2} (\bar{q}_i \gamma_\lambda q_i) (\bar{q}_k \gamma_\lambda q_j) \\ &\quad - g_w^2 (m_w^2 - \hat{t})^{-1} [\bar{q}_i \gamma_\lambda (1 + \gamma_5) q_i] [\bar{q}_k \gamma_\lambda (1 + \gamma_5) q_j]. \end{aligned} \quad (4.1)$$

In Eq. (4.1) q_i , q_j , \bar{q}_k , and \bar{q}_l are the parton spinors, g_w is the weak coupling constant, and m_w is the mass of the hypothetical W boson.

In writing Eq. (4.1) we have assumed that $F^2(\hat{t}) = (1 - \hat{t}/B)^{-2}$ represents an effective modification of the strong interaction amplitude and hence should not appear in the expression for the weak contribution. It is possible, however, that $F^2(\hat{t})$ represents a parton form factor, as we have discussed earlier, in which case the factor $(1 - \hat{t}/B)^{-2}$ should appear in both terms in Eq. (4.1). It is interesting that one may be able to distinguish between these

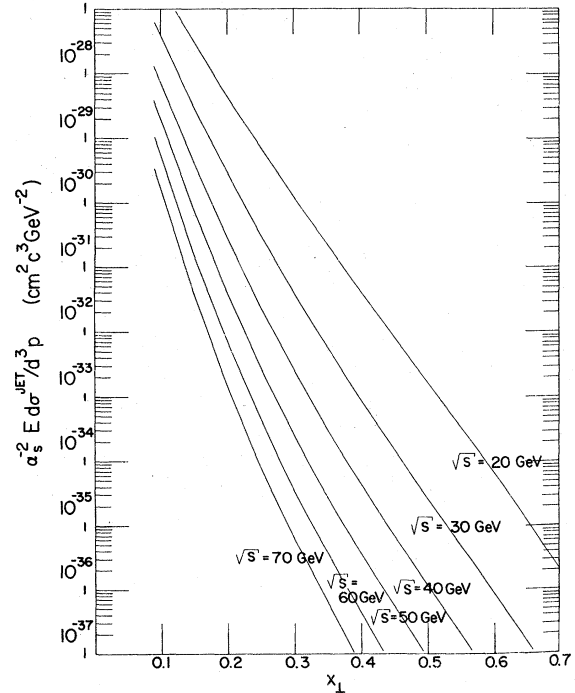


FIG. 21. Invariant cross section (divided by α_s^2) for the production of particle jets in the EG model at $\theta_{\text{c.m.}} = 90^\circ$.

two interpretations of the *strong* amplitude in (4.1) by examining the *weak* effects expected on the basis of each assumption: If $F^2(\hat{t})$ represents a parton form factor, then its inclusion in the second term in Eq. (4.1) will reduce the size of the weak effects relative to what would be expected if this term is omitted. A preliminary discussion of this point has been given elsewhere,²⁸ and calculations along this line are presently under way.

Note added in manuscript. (1) After submitting

this manuscript we learned of a revision in the data of Cronin *et al.*, Ref. 14. A preliminary analysis of the new data²⁹ indicates an improved agreement between the present model and experiment. A detailed comparison of the new data with the present theory will be given elsewhere. (2) A phenomenological hard-scattering parton model similar to ours has been published recently by Field and Feynman.³⁰ (3) A brief discussion of the EG model is given in Ref. 28.

*Work supported in part by the U.S. Energy Research and Development Administration.

¹E. Fischbach and G. W. Look, Phys. Rev. D **13**, 752 (1976).

²L. L. Frankfurt and V. B. Kopeliovich, Nucl. Phys. **B103**, 360 (1976).

³J. Missimer, L. Wolfenstein, and J. Gunion, Nucl. Phys. **B111**, 20 (1976).

⁴K. H. Craig, Nucl. Phys. **B109**, 156 (1976).

⁵E. M. Henley and F. R. Krejs, Phys. Rev. D **11**, 605 (1975).

⁶S. M. Berman, J. D. Bjorken, and J. B. Kogut, Phys. Rev. D **4**, 3388 (1971).

⁷S. D. Ellis and M. B. Kislinger, Phys. Rev. D **9**, 2027 (1974).

⁸M. S. Chanowitz and S. D. Drell, Phys. Rev. Lett. **30**, 807 (1973).

⁹R. Blankenbecler, S. J. Brodsky, and J. F. Gunion, Phys. Rev. D **12**, 3469 (1975); R. Blankenbecler, S. J. Brodsky, J. F. Gunion, and R. Savit, *ibid.* **10**, 2153 (1974).

¹⁰F. W. Büsser, L. Camilleri, L. DiLella, G. Gladding, A. Placci, B. G. Pope, A. M. Smith, J. K. Yoh, E. Zavattini, B. J. Blumenfeld, L. M. Lederman, R. L. Cool, L. Litt, and S. L. Segler, Phys. Lett. **46B**, 471 (1973).

¹¹F. W. Büsser, L. Camilleri, L. DiLella, B. G. Pope, A. M. Smith, B. J. Blumenfeld, S. N. White, A. F. Rothenberg, S. L. Segler, M. J. Tannenbaum, M. Banner, J. B. Cheze, J. L. Hamel, H. Kasha, J. P. Pansart, G. Smadja, J. Teiger, H. Zacccone, and A. Zylberstejn, Phys. Lett. **55B**, 232 (1975). This paper notes that the data of Ref. 10 should be renormalized by multiplying by 0.72.

¹²B. Alper, H. Bøggild, P. Booth, L. J. Carroll, G. von Dardel, G. Damgaard, B. Duff, J. N. Jackson, G. Jarlskog, J. Jönsson, A. Klovning, L. Leistam, E. Lillethun, S. Olgaard-Nielsen, M. Prentice, and J. M. Weiss, Nucl. Phys. **B87**, 19 (1975).

¹³B. Alper, H. Bøggild, P. Booth, F. Bulos, L. J. Carroll, G. von Dardel, G. Damgaard, B. Duff, K. H. Hanson, F. Heymann, J. N. Jackson, G. Jarlskog, L. Jönsson, A. Klovning, L. Leistam, E. Lillethun, E. Lohse, G. Lynch, G. Manning, S. Olgaard-Nielsen, K. Potter, M. Prentice, D. Quarrie, P. Sharp, S. Sharrock, and J. M. Weiss, Nucl. Phys. **B100**, 237 (1975).

¹⁴J. W. Cronin, H. J. Frisch, M. J. Shochet, J. P. Boymond, P. A. Piroué, and R. L. Sumner, Phys. Rev. Lett. **31**, 1426 (1973); Phys. Rev. D **11**, 3105 (1975).

¹⁵R. C. Hwa, A. J. Spiessbach, and M. J. Teper, Phys. Rev. Lett. **36**, 1418 (1976).

¹⁶For π^\pm , π^0 , K^\pm , p , n production the observed particle has the correct quantum numbers to allow it to be produced from the decay of a u or d valence quark in the incident particles. However, K^- and \bar{p} production can arise only from \bar{u} , \bar{d} , or s quarks and hence the *entire* K^- and \bar{p} contributions in the EG model come from the sea of the incident particles. Nonetheless, the quark-antiquark annihilation diagram can be neglected in comparison to the contribution in which the quark-antiquark scattering takes place via gluon exchange. To make this plausible, consider the usual annihilation and exchange contributions to Bhabha scattering, in analogy to Eqs. (2.9) and (2.10). To handle the pole at $\hat{s}=B$ in $F(\hat{s})$, the replacement $(\hat{s}-B)^2 \rightarrow (\hat{s}-B)^2 + \Gamma^2 B$ is made. Γ represents the width of the fictitious particle of mass B which generates the "form factor" $F(\hat{s})$, and arises because of the existence of "decay" channels such as $B \rightarrow q\bar{q}$. Numerical evaluation of the resulting expressions for the annihilation and exchange contributions to $E_c d\sigma/d^3p_c$ then shows that the exchange contribution is roughly 10^2 – 10^3 larger than the annihilation contribution for values of Γ in the range $0.1 \leq \Gamma/\sqrt{B} \leq 1$. Even without the form factors the annihilation contribution is smaller than the exchange contribution, as one can infer from an analysis of Fig. 3 of Ref. 7. In summary, the $q\bar{q}$ annihilation contribution can be neglected both for π^\pm , π^0 , K^\pm , p , n production (where the sea contribution is small compared to the valence contribution), and also for K^- , \bar{p} production (where the sea gives the principal contribution).

¹⁷J. Kuti and V. F. Weisskopf, Phys. Rev. D **4**, 3418 (1971).

¹⁸R. McElhaney and S. F. Tuan, Phys. Rev. D **8**, 2267 (1973); and Nucl. Phys. **B72**, 487 (1974); J. Okada, S. Pakvasa, and S. F. Tuan, Lett. Nuovo Cimento **16**, 55 (1976). The last reference listed here presents a comparison of the MKW functions and other proposed forms of the parton distribution functions of the proton, concluding that the modified Kuti-Weisskopf functions are unique in surviving recent experimental tests of the distributions. Other forms of the distributions use essentially the same form for the valence contribution, but disagree on the sea distributions, which affects primarily the K^- and \bar{p} predictions. We have found that the MKW distributions provide the best description of the K^- and \bar{p} cross sections, with the use of other distributions predicting a fall of the cross

section with x_1 which is somewhat more rapid than that observed experimentally.

¹⁹J. J. Sakurai, *Advanced Quantum Mechanics* (Addison-Wesley, Reading, Mass., 1967), p. 258.

²⁰Our calculation using the MKW distribution functions gives $\langle \bar{d} \rangle < 0.1 \langle u \rangle$ in the relevant kinematic region.

²¹R. P. Feynman, *Photon-Hadron Interactions* (Benjamin, Reading, Mass., 1972), p. 149.

²²These constants were evaluated by taking the average of the normalizations calculated for each experimental point, ignoring the experimental error.

²³A. R. Erwin, E. H. Harvey, R. J. Loveless, M. A. Thompson, D. R. Winn, V. E. Barnes, D. D. Carmony, R. S. Christian, A. F. Garfinkel, W. M. Morse, and L. K. Rangan, *Phys. Rev. Lett.* **36**, 636 (1976).

²⁴F. W. Büsler, L. Camilleri, L. DiLella, B. G. Pope, A. M. Smith, B. J. Blumenfeld, S. N. White, A. F. Rothenberg, S. L. Segler, M. J. Tannenbaum, M. Banner, J. B. Chèze, H. Kasha, J. P. Pansart, G. Smadja, J. Teiger, H. Zacccone, and A. Zylberstejn, *Phys. Lett.* **61B**, 309 (1976).

²⁵When $n = n(x_1)$ is not a constant, Eq. (3.5) cannot, of

course, be understood to be an equation in the usual sense, since this would require the existence of functions $g_n(x_1)$ and $h_n(x_1)$ with continuously changing dimensions. The parametrization of Eq. (3.5) should be understood to mean that $n(x_1)$ is the effective exponent obtained by measuring the invariant cross section in a small neighborhood around a particular x_1 and fitting to the indicated functional form. As x_1 varies, both n and the functions $g_n(x_1)$ and $h_n(x_1)$ vary. Thus g_n and h_n are actually *different functions* with different dimensions for each n .

²⁶J. D. Bjorken, *Acta Phys. Polon.* **B5**, 893 (1974).

²⁷S. D. Ellis, M. Jacob, and P. V. Landshoff, *Nucl. Phys.* **B108**, 93 (1976).

²⁸E. Fischbach and G. W. Look, in *High Energy Physics with Polarized Beams and Targets*, proceedings of the Symposium, Argonne, 1976, edited by M. L. Marshak (A.I.P., New York, 1976), p. 258.

²⁹D. Antreasyan *et al.*, *Phys. Rev. Lett.* **38**, 112 (1977); **38**, 115 (1977).

³⁰R. D. Field and R. P. Feynman, *Phys. Rev. D* **15**, 2590 (1977).